

ON THE DETERMINATION OF THE CRACK ARREST- TOUGHNESS

J. F. Kalthoff, J. Beinert, S. Winkler and J. Blauel*

INTRODUCTION

By analogy with the K_{Ic} -criterion for crack initiation a crack arrest criterion may be formulated: a running crack is arrested if the stress intensity factor K_I falls below a critical threshold value, the crack arrest toughness K_{Ia} . This statement is only of any value in design or safety analysis if it can be shown that K_{Ia} is a material property, i.e. that it is independent of the crack velocity during the previous propagation phase and does not depend on the geometrical parameters of the specimen or component.

Usually the determination of the crack arrest toughness K_{Ia} is based on a static analysis of the crack arrest process. Crosley and Ripling [1], for instance, assume that all dynamic effects through stress waves or structural vibrations become negligible. Then the arrest conditions are adequately described by the static stress-strain field following crack arrest and crack arrest toughness of the material can be determined.

Theoretical considerations and calculations by Hahn et al. [2] on the energetics during the crack propagation predict, that - depending on the prevailing geometrical and material conditions - dynamic effects may have a remarkable influence on the crack arrest process. The authors therefore conclude that in principle statically determined crack arrest toughness values cannot represent a true material property and that it is necessary to consider the total process of crack initiation and propagation in order to predict correctly crack arrest for any specific case.

Dynamic effects on the crack arrest process are also predicted from theoretical analyses of Shmueli [3] and Nilsson [4] and confirmed by experiments of Kalthoff et al. [5].

In this paper it is shown that crack arrest toughness values K_{Ia} representing a true material property do exist. They can be determined from the actual dynamic stress intensity factors prevailing at arrest. Results for a model material Araldit B and steel will be discussed.

EXPERIMENTAL

The experiments were performed in DCB specimens of different dimensions (see Figure 1) which were loaded under conditions of fixed grips by a wedge driven between the two bolts. Machined starter notches with different root radii were used to initiate cracks at stress intensity factors K_{Iq} larger than the fracture toughness K_{Ic} and to achieve different crack velocities. The materials investigated were an epoxy resin, Araldite

*Fraunhofer-Gesellschaft, Institut für Festkörpermechanik,
7800 Freiburg i.Br., Federal Republic of Germany.

B, and two types of steel, a high strength steel, HFX 760, (18 Ni grade 300 maraging) and a reactor steel 22 Ni Mo Cr 3 7 (similar to ASTM 508 C1 2) in hardened condition.

The stress intensity factors of the arresting cracks were measured during the propagation phase, at the moment of arrest and after arrest. For the measurement of the stress intensity factors - and also of the crack velocities - the shadow optical method after Manogg [5, 6] was used in combination with a Cranz-Schardin high speed camera. This method - originally developed for transparent materials - is applied here for the steel experiments in reflection.

Values of stress intensity factors can be derived shadowoptically when linear elastic behaviour obtains (for Araldite and the maraging steel); for large plastic deformations at the crack tip (as with the reactor steel) at least information about the crack velocity is delivered. Figure 2 shows the characteristic shadow patterns at the crack tip in an Araldite specimen (in transmission) and in a steel specimen (in reflection).

RESULTS

Figure 3 shows the shadowoptically measured dynamic stress intensity factor K_{Ia}^{dyn} together with the corresponding crack length a as a function of time. For comparison the static stress intensity factor K_{Ia}^{stat} is given in a diagram which was calculated for the prevailing geometrical conditions from the measured beam deflection at the loading line using the conventional formula (Kanninen [7]). The following differences between the dynamic and the static case are apparent:

- At the beginning of the crack propagation phase the actual dynamic stress intensity factor K_{Ia}^{dyn} is smaller than the corresponding statically determined stress intensity factor K_{Ia}^{stat} .
- In a later phase of the crack propagation K_{Ia}^{dyn} is larger than K_{Ia}^{stat} .
- Also the stress intensity factor in the moment of arrest, K_{Ia}^{dyn} , is significantly larger than the corresponding statically determined K_{Ia}^{stat} .
- After arrest K_{Ia}^{dyn} decays slowly towards the static value K_{Ia}^{stat} in a damped oscillation.

These results prove, that for DCB specimens dynamic effects are not negligible and must be taken into account in a crack arrest analysis. In Figure 4 for some experiments, which are representative of different crack velocity ranges, the measured stress intensity factor K_{Ia}^{dyn} and for comparison the statically determined K_{Ia}^{stat} are plotted versus crack length a . The lower part of the diagram shows the corresponding crack velocities v . The differences between the K_{Ia}^{dyn} curve and the K_{Ia}^{stat} curve are in principle the same as in Figure 3, but obviously for the experiments with higher maximum velocities v_{max} these differences - that means the dynamic effects - become larger.

It is important to note, that in Figure 4 the experimentally observed stress intensity factors in the moment of arrest K_{Ia}^{dyn} (large black circles) are apparently constant for all experiments with different velocity histories prior to arrest. On the contrary, the values K_{Ia}^{stat} (black rhombi) determined from the static analysis depend on these velocity histories.

The velocity independence of K_{Ia}^{dyn} is shown more clearly in Figure 5: For several experiments the values of K_{Ia}^{dyn} and K_{Ia}^{stat} are plotted against the maximum crack velocity v_{max} attained in the respective experiment. Additionally the results from DCB specimens of different dimensions are given. Obviously one can conclude:

- Whereas the statically determined values K_{Ia}^{stat} depend on the velocity the actual observed values K_{Ia}^{dyn} are independent of the velocity and, moreover, the specimen dimensions. The value of K_{Ia}^{dyn} therefore is a true material property and can be considered as the crack arrest toughness.

For Araldite B K_{Ia}^{dyn} lies slightly below (but within the error band) of the crack initiation toughness K_{Ic} . For steels, which in general show a higher strain rate sensitivity, a more pronounced difference is expected between K_{Ia}^{dyn} and the true crack arrest toughness. Experiments following the guide line of the model investigations are on the way and will be reported during the conference. Results like that in Figure 6 will be discussed not only in terms of a fracture mechanics stress analysis but under special consideration of the material conditions and the velocity induced fracture mode transition.

CONCLUSIONS

The experimental results demonstrate, that the dynamic stress intensity factor K_{Ia}^{dyn} - determined in the moment of arrest - represents the crack arrest toughness: It is a true material property, independent of the preceding crack velocity and of the specimen size. This K_{Ia}^{dyn} value differs significantly from the values obtained following the static concept. Therefore the results confirm the assumptions of the dynamic concept mentioned in the introduction.

ACKNOWLEDGEMENT

The work was funded by the Bundesministerium für Forschung und Technologie of the Federal Republic of Germany.

REFERENCES

1. CROSLLEY, R. P. and RIPLING, E. J., Proc. 2nd Int. Conf. on Pressure Vessel Technology, San Antonio, Texas, ASME, 1973, 995-1005.
2. HAHN, G. T., HOAGLAND, R. G., KANNINEN, M. F., ROSENFELD, A. R. and SEJNOHA, R., SSC-Progress Rep. on Project SR 201, Battelle, Columbus Laboratories, Columbus, Ohio, 1973.
3. SHMUELY, M., "Analysis of Fast Fracture and Crack Arrest by Finite Differences", to be published in J. Appl. Mech., 1976.
4. NILSSON, F., Rapport 18, Division of Strength of Materials and Solid Mechanics, The Royal Institute of Technology, Stockholm, Sweden, 1976.
5. KALTHOFF, J. F., BEINERT, J. and WINKLER, S., Symp. on Fast Fracture and Crack Arrest, Chicago, Illinois, 1976.
6. MANOGG, P., Proc. Int. Conf. on Physics of Non-Crystalline Solids, Delft, Netherlands, 1964, 481.
7. KANNINEN, M. F., Int. J. Fracture, 9, 1973, 83.

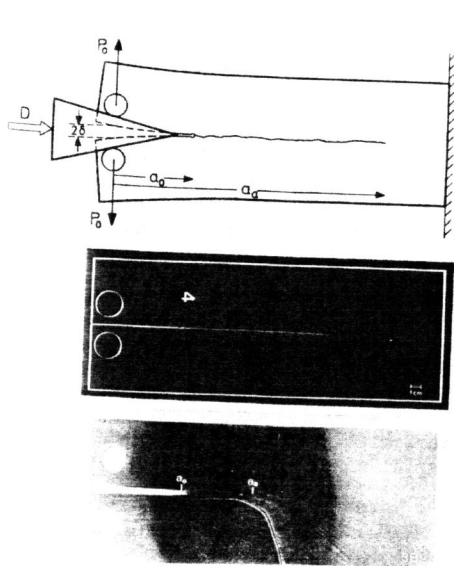


Figure 1 Principle of the Crack Arrest Test Arrangement (Upper); A Broken Araldite B Specimen (Middle); a Tested Steel Specimen (22 Ni Mo Cr 3 7, Hardened) which has been Subsequently Broken Open (Lower)

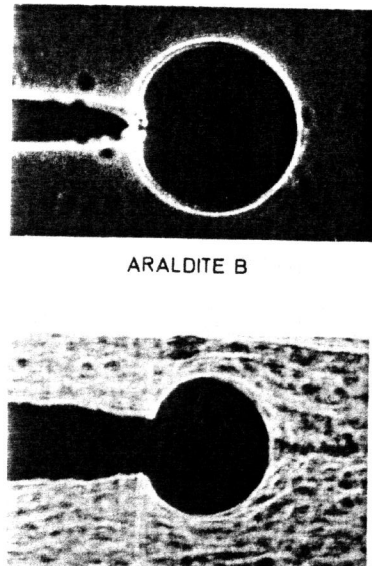


Figure 2 Shadow Patterns at Araldite B (Upper) in Transmission and HF X 760 (Lower) in Reflection

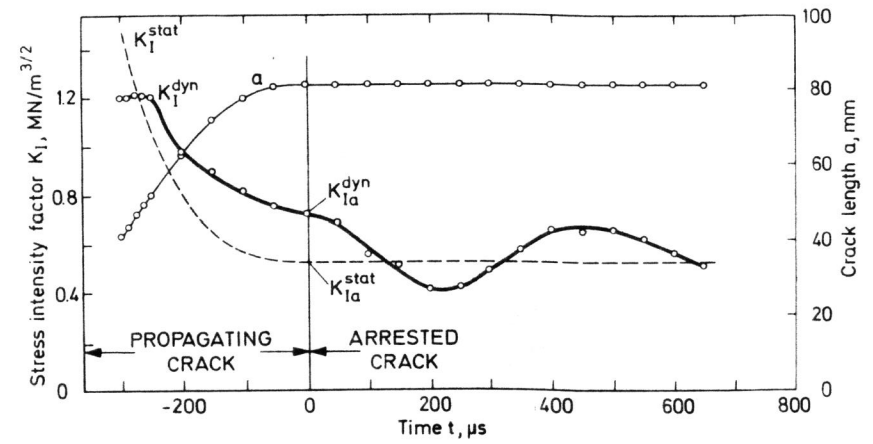


Figure 3 Stress Intensity Factors and Crack Length versus Time Before and after Crack Arrest. Specimen: Araldite B, 134 x 53 x 10 mm³, Maximum Crack Velocity v_{max} = 270 m/sec

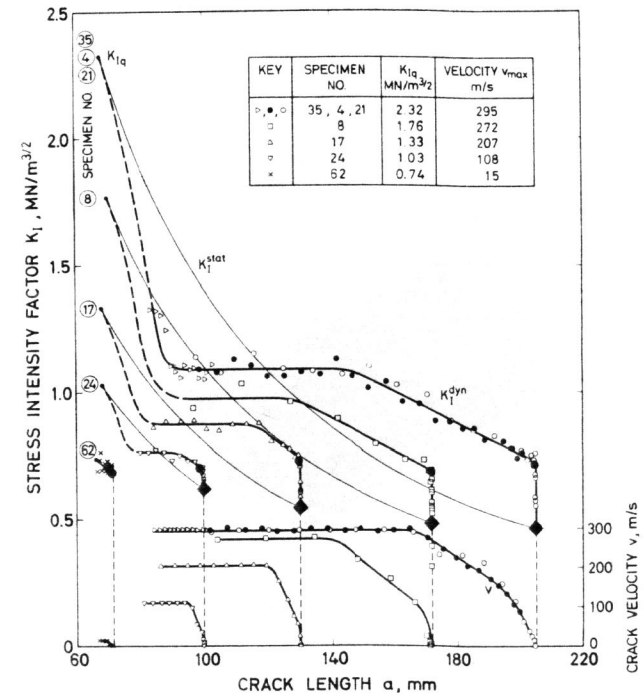


Figure 4 Stress Intensity Factors and Crack Velocities for Arresting Cracks versus Crack Length. Specimen: Araldite B, 321 x 127 x 10 mm³

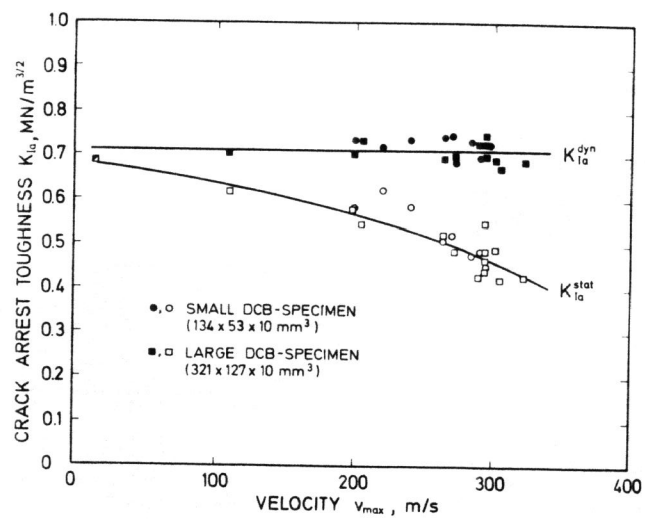


Figure 5 The Velocity Dependence of the Observed Dynamic and the Statically Determined Crack Arrest Toughness Values

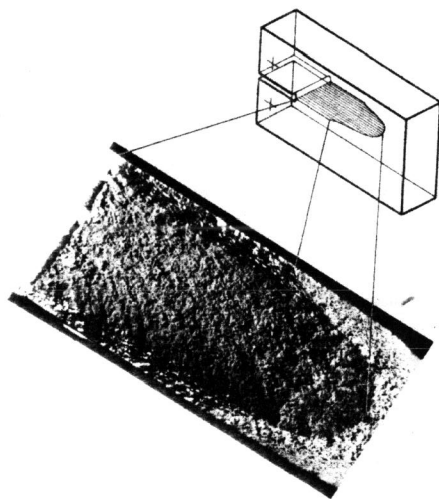


Figure 6 Fracture Surface from an Arrest Experiment in Hardened Reactor Steel at Room Temperature (Specimen Thickness 25 mm)